JCTC Journal of Chemical Theory and Computation

Article

pubs.acs.org/JCTC

Analytic Energy Gradients and Spin Multiplicities for Orbital-Optimized Second-Order Perturbation Theory with Density-Fitting Approximation: An Efficient Implementation

Uğur Bozkaya*

Department of Chemistry, Atatürk University, Erzurum 25240, Turkey

Department of Chemistry, Middle East Technical University, Ankara 06800, Turkey

Supporting Information

ABSTRACT: An efficient implementation of analytic energy gradients and spin multiplicities for the density-fitted orbital-optimized second-order perturbation theory (DF-OMP2) [Bozkaya, U. *J. Chem. Theory Comput.* **2014**, *10*, 2371−2378] is presented. The DF-OMP2 method is applied to a set of alkanes, conjugated dienes, and noncovalent interaction complexes to compare the cost of single point analytic gradient computations with the orbital-optimized MP2 with the resolution of the identity approach (OO-RI-MP2) [Neese, F.; Schwabe, T.; Kossmann, S.; Schirmer, B.; Grimme, S. *J. Chem. Theory Comput.* **2009**, *5*, 3060−3073]. Our results demonstrate that the DF-OMP2 method provides substantially lower computational costs for analytic gradients than OO-RI-MP2. On average, the cost of DF-OMP2 analytic gradients is 9−11 times lower than that of OO-RI-MP2 for systems considered. We also consider aromatic bond dissociation energies, for which MP2 provides poor reaction energies. The DF-OMP2 method exhibits a substantially better performance than MP2, providing a mean absolute error of 2.5 kcal mol^{-1}, which is more than 9 times lower than that of MP2 (22.6 kcal mol^{-1}). Overall, the DF-OMP2 method appears very helpful for electronically challenging chemical systems such as free radicals or other cases where standard MP2 proves unreliable. For such problematic systems, we recommend using DF-OMP2 instead of the canonical MP2 as a more robust method with the same computational scaling.

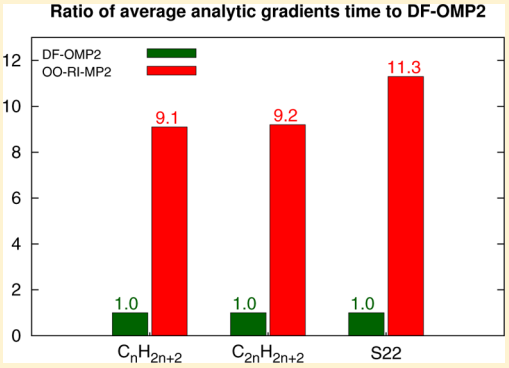

1. INTRODUCTION

Orbital-optimized methods, in which the energy of some correlated wave function is minimized with respect to orbital rotations, have considerable importance in modern computational chemistry.[1−23] Previous studies demonstrated that the orbital-optimized Møller−Plesset perturbation (MP) theory and coupled-cluster (CC) methods are very helpful for the study of difficult chemical systems, such as symmetry-breaking problems,[2−4,7−9] transition states,[6,13,20] free radicals,[6−8,13,20] bond-breaking problems,[5,24,25] open-shell noncovalent interactions,[10] and direct computation of ionization potentials and electron affinities.[11,12]

Tensor factorizations of the four-index electron repulsion integrals (ERIs) have been of great interest for electron correlation methods. One of the commonly used approximations is the density fitting (DF), which is also known as the resolution of the identity (RI).[14,26−34] In the DF approximation, the four-index two-electron integrals (TEIs) are expressed in terms of the three-index tensors. Another integral factorization method is the partial Cholesky decomposition (CD) of the TEI tensor.[35−38] The DF and CD approaches are very successful to reduce the storage cost of ERIs, as well as the computational time. In the DF approach, integrals of the primary basis set are expressed in terms of a preconstructed auxiliary basis set, whereas in the CD method the three-index tensors are directly generated from the primary basis set. However, analytic gradients cannot be computed with the CD approximation unless one employs an approach such as that of Aquilante et al.[39]

The DF approach was used for the orbital-optimized second-order Møller−Plesset perturbation theory (OMP2), which is denoted as OO-RI-MP2.[20] However, Neese et al.[20] employed the DF approach only for the correlation energy but not for the reference contribution of the OMP2 energy. In our recent study,[14] an efficient implementation of the orbital-optimized second-order perturbation theory with the density-fitting (DF-OMP2) and Cholesky decomposition (CD-OMP2) approaches are presented. It was demonstrated that the DF-OMP2 method provides substantially (7−11 times on average) lower computational costs than OO-RI-MP2.[14]

In this research, analytic energy gradients and spin multiplicities for the DF-OMP2 method are presented (analytic gradients of the CD-OMP2 method are not implemented). The DF-OMP2 method is applied to several chemical systems where standard MP2 has difficulties, such as aromatic bond

Received: July 18, 2014
Published: September 17, 2014

   dx.doi.org/10.1021/ct500634s | *J. Chem. Theory Comput.* 2014, 10, 4389−4399

dissociation energies. The equations presented have been implemented in a new computer code and added to the DFOCC module of the PSI4 package.[40] Both restricted and unrestricted formalisms are implemented. The computational time for single point analytic gradients of the DF-OMP2 method is compared with that of OO-RI-MP2.[20]

2. THEORETICAL APPROACH

2.1. Density-Fitting. In the DF approach, the atomic-orbital (AO) basis TEIs are approximated as[26,27]

$$(\mu\nu|\lambda\sigma)_{\mathrm{DF}} = \sum_{\mathrm{Q}}^{N_{\mathrm{aux}}} b_{\mu\nu}^{\mathrm{Q}} b_{\lambda\sigma}^{\mathrm{Q}} \tag{1}$$

the DF factor $b_{\mu\nu}^{\mathrm{Q}}$ is defined as[26,27]

$$b_{\mu\nu}^{\mathrm{Q}} = \sum_{P}^{N_{\mathrm{aux}}} (\mu\nu|P)[\mathbf{J}^{-1/2}]_{PQ} \tag{2}$$

where

$$(\mu\nu|P) = \int\int \chi_{\mu}(\mathbf{r}_1)\chi_{\nu}(\mathbf{r}_1)\frac{1}{r_{12}}\varphi_{P}(\mathbf{r}_2)\mathrm{d}\mathbf{r}_1\mathrm{d}\mathbf{r}_2 \tag{3}$$

and

$$J_{\mathrm{PQ}} = \int\int \varphi_{\mathrm{P}}(\mathbf{r}_1)\frac{1}{r_{12}}\varphi_{\mathrm{Q}}(\mathbf{r}_2)\mathrm{d}\mathbf{r}_1\mathrm{d}\mathbf{r}_2 \tag{4}$$

where $\{\chi_{\mu}(\mathbf{r})\}$ and $\{\varphi_{P}(\mathbf{r})\}$ are members of the primary and auxiliary basis sets, respectively.

The molecular orbital (MO) basis integrals can be approximated as

$$(pq|rs)_{\mathrm{DF}} = \sum_{\mathrm{Q}}^{N_{\mathrm{aux}}} b_{pq}^{\mathrm{Q}} b_{rs}^{\mathrm{Q}} \tag{5}$$

where b_{pq}^{Q} is a MO basis DF factor.

2.2. DF-OMP2 Energy. Let us consider the DF-OMP2 energy first.[14] The next section will present the DF-OMP2 analytic energy gradients. For the orbital indexing the conventional notation is used: *i,j,k,l,m,n* for occupied orbitals; *a,b,c,d,e,f* for virtual orbitals; and *p,q,r,s,t,u* for general spin orbitals. For DF-OMP2, the following variational energy functional (Lagrangian) can be written[3,7,14]

$$\begin{aligned}\tilde{E}(\kappa) = {} & \langle 0|\hat{H}^{\kappa}|0\rangle + \langle 0|(\hat{W}_{N}^{\kappa}\hat{T}_{2}^{(1)})_{c}|0\rangle \\ & + \langle 0|\{\hat{\Lambda}_{2}^{(1)}(\hat{f}_{N}^{\kappa}\,\hat{T}_{2}^{(1)} + \hat{W}_{N}^{\kappa})_{c}\}_{c}|0\rangle\end{aligned} \tag{6}$$

where $\hat{H}^{\kappa}$, $\hat{f}_{N}^{\kappa}$, $\hat{W}_{N}^{\kappa}$, and $\hat{H}_{N}^{\kappa}$ are transformed operators

$$\hat{H}^{\kappa} = e^{-\hat{K}}\hat{H}e^{\hat{K}} \tag{7}$$

$$\hat{f}_{\mathrm{N}}^{\kappa} = e^{-\hat{K}}\hat{f}_{\mathrm{N}}^{d}\,e^{\hat{K}} \tag{8}$$

$$\hat{W}_{\mathrm{N}}^{\kappa} = e^{-\hat{K}}\hat{W}_{\mathrm{N}}e^{\hat{K}} \tag{9}$$

$$\hat{H}_{\mathrm{N}}^{\kappa} = \mathrm{e}^{-\hat{K}}\hat{H}_{\mathrm{N}}e^{\hat{K}} \tag{10}$$

where $\hat{H}$ is the Hamiltonian operator, $\hat{H}_{\mathrm{N}}$ is the normal ordered Hamiltonian operator, and $\hat{f}_{\mathrm{N}}$ and $\hat{W}_{\mathrm{N}}$ are one- and two-electron components of the normal ordered Hamiltonian operator,[41,42] and $e^{\hat{K}}$ is the orbital rotation operator[3,7,14,43−45]

$$\hat{K} = \sum_{p,q} K_{pq}\hat{p}^{\dagger}\hat{q} = \sum_{p>q} \kappa_{pq}(\hat{p}^{\dagger}\hat{q} - \hat{q}^{\dagger}\hat{p}) \tag{11}$$

where κ_{pq} are the orbital rotation parameters, $\hat{p}^{\dagger}$ and $\hat{q}$ are the creation and annihilation operators, respectively.

The first and second derivatives of the Lagrangian with respect to κ (at $\kappa = 0$) can be written as

$$w_{pq} = \left.\frac{\partial\tilde{E}}{\partial\kappa_{pq}}\right|_{\kappa=0} \tag{12}$$

$$A_{pq,rs} = \left.\frac{\partial^2\tilde{E}}{\partial\kappa_{pq}\partial\kappa_{rs}}\right|_{\kappa=0} \tag{13}$$

Then the Lagrangian can be expanded up to second-order as follows:

$$\tilde{E}^{(2)}(\kappa) = \tilde{E}^{(0)} + \kappa^{\dagger}\mathbf{w} + \frac{1}{2}\kappa^{\dagger}\mathbf{A}\kappa \tag{14}$$

where $\mathbf{w}$ is the MO gradient vector, κ is the MO rotation vector, and $\mathbf{A}$ is the MO Hessian matrix. Hence, minimizing the Lagrangian with respect to κ yields

$$\kappa = -\mathrm{A}^{-1}\mathrm{w} \tag{15}$$

This final equation is just the usual Newton−Raphson equation. Hence, the orbitals are rotated until the convergence. For a more detailed discussion of our orbital optimization algorithm one can refer to our recent study.[14]

2.3. Geometry Dependent Transformations. Let us discuss the geometry dependent transformation of orbitals, hence molecular integrals, first.[7−9,46] Consider a molecular system at a reference geometry $\mathbf{x}_0$. The converged MOs at $\mathbf{x}_0$ can be expressed in terms of atomic orbitals (AO) $\chi(\mathbf{x}_0)$

$$\phi_{p}(\mathbf{x}_0) = \sum_{\mu} C_{\mu p}(\mathbf{x}_0)\chi_{\mu}(\mathbf{x}_0) \tag{16}$$

where $\mathbf{C}(\mathbf{x}_0)$ is the MO coefficient matrix. Orbitals are orthonormal at $\mathbf{x}_0$

$$\langle\phi_{p}(\mathbf{x}_0)|\phi_{q}(\mathbf{x}_0)\rangle = \delta_{pq} \tag{17}$$

In order to describe the change in the MOs at perturbed geometries, it is convenient to introduce a new orbital basis $\phi(\mathbf{x})$ called as *unmodified molecular orbital* (UMO) basis, which is expressed in terms of the optimized MO coefficients $\mathbf{C}(\mathbf{x}_0)$ at the reference geometry[47,48]

$$\phi_{p}(\mathbf{x}) = \sum_{\mu} C_{\mu p}(\mathbf{x}_0)\chi_{\mu}(\mathbf{x}) \tag{18}$$

The UMO basis is orthonormal at $\mathbf{x}_0$, but other geometries it is not. Therefore, it is appropriate to introduce a connection matrix $\mathbf{T}(\mathbf{x})$, which orthonormalizes the UMO basis at arbitrary geometries[47−49]

$$\mathbf{T}(\mathbf{x})^{\dagger}\mathbf{S}(\mathbf{x})\mathbf{T}(\mathbf{x}) = 1 \tag{19}$$

where $\mathbf{S}(\mathbf{x})$ is the overlap matrix. The most common choice for the connection matrix $\mathbf{T}(\mathbf{x})$ is the Löwdin's symmetric connection[47−49]

$$\mathbf{T}(\mathbf{x}) = \mathbf{S}(\mathbf{x})^{-1/2} \tag{20}$$

the symmetric orbital connection matrix defines a new geometry-dependent basis $\tilde{\boldsymbol{\phi}}(\mathbf{x})$, which is called as *orthonormalized molecular orbital* (OMO) basis

$$\tilde{\boldsymbol{\phi}}(\mathbf{x}) = \boldsymbol{\phi}(\mathbf{x})\mathbf{S}(\mathbf{x})^{-1/2} \tag{21}$$

the OMO basis is orthonormal at all geometries, and one can readily verify that

$$\tilde{\mathbf{S}}(\mathbf{x}) = 1 \tag{22}$$

In the OMO basis, the Hamiltonian operator can be written as follows

$$\hat{H}(\mathbf{x}) = \sum_{p,q} \tilde{h}_{pq}(\mathbf{x})\hat{p}^{\dagger}\hat{q} + \frac{1}{4}\sum_{p,q,r,s} \tilde{g}_{pqrs}(\mathbf{x})\hat{p}^{\dagger}\hat{q}^{\dagger}\hat{s}\hat{r} \tag{23}$$

where $\tilde{g}_{pqrs}$ is the antisymmetrized two-electron integral in the OMO basis

$$\tilde{g}_{pqrs} = \langle \tilde{p}\tilde{q}||\tilde{r}\tilde{s}\rangle_{\mathrm{DF}} \tag{24}$$

one- and two-electron integrals $\tilde{h}_{pq}(\mathbf{x})$ and $\tilde{g}_{pqrs}(\mathbf{x})$ in the OMO basis can be expressed in the UMO basis as follows

$$\tilde{\mathbf{h}}(\mathbf{x}) = \mathbf{S}(\mathbf{x})^{-1/2\dagger}\mathbf{h}(\mathbf{x})\mathbf{S}(\mathbf{x})^{-1/2} \tag{25}$$

$$\tilde{g}_{pqrs}(\mathbf{x}) = \sum_{tuvw} S_{tp}(\mathbf{x})^{-1/2}S_{uq}(\mathbf{x})^{-1/2}S_{vr}(\mathbf{x})^{-1/2} \times S_{ws}(\mathbf{x})^{-1/2}g_{tuvw}(\mathbf{x}) \tag{26}$$

The first derivative of molecular integrals $\tilde{h}_{pq}(\mathbf{x})$ and $\tilde{g}_{pqrs}(\mathbf{x})$ at the reference geometry is also of particular interest. Differentiating one- and two-electron integrals with respect to $\mathbf{x}$ at $\mathbf{x}_0$ we obtain[45,47−51]

$$\tilde{\mathbf{h}}^{\mathbf{x}} = \mathbf{h}^{\mathbf{x}} - \frac{1}{2}\{\mathbf{S}^{\mathbf{x}}, \mathbf{h}\} \tag{27}$$

$$\tilde{\mathbf{g}}^{\mathbf{x}} = \mathbf{g}^{\mathbf{x}} - \frac{1}{2}\{\mathbf{S}^{\mathbf{x}}, \mathbf{g}\} \tag{28}$$

where $\{\mathbf{A},\mathbf{B}\}$ denotes the anticommutator, and $\mathbf{S}^{\mathbf{x}}$, $\mathbf{h}^{\mathbf{x}}$, and $\mathbf{g}^{\mathbf{x}}$ are the *skeleton (core)* derivative integrals,[52] which are corresponding to the purely AO derivative parts

$$S^{x}_{pq} = \sum_{\mu\nu} C_{\mu p}C_{\nu q}S^{x}_{\mu\nu} \tag{29}$$

$$h^{x}_{pq} = \sum_{\mu\nu} C_{\mu p}C_{\nu q}h^{x}_{\mu\nu} \tag{30}$$

$$g^{x}_{pqrs} = \sum_{\mu\nu\lambda\sigma} C_{\mu p}C_{\nu q}C_{\lambda r}C_{\sigma s}\langle\mu\nu||\lambda\sigma\rangle^{x}_{\mathrm{DF}} \tag{31}$$

2.4. DF-OMP2 Gradient. For the DF-OMP2 wave function we can write the following Lagrangian

$$\tilde{E} = \langle 0|\hat{H}|0\rangle + \langle 0|(\hat{W}_{\mathrm{N}}\hat{T}^{(1)}_{2})_{c}|0\rangle + \langle 0|\{\hat{\Lambda}^{(1)}_{2}(\hat{f}^{d}_{\mathrm{N}}\hat{T}^{(1)}_{2} + \hat{W}_{\mathrm{N}})_{c}\}_{c}|0\rangle \tag{32}$$

the gradient of the energy can be obtained from the first derivative of the Lagrangian in eq 32 as follows[49,53−55]

$$\left.\frac{\mathrm{d}E}{\mathrm{d}x}\right|_{x=x_0} = \left.\frac{\partial\tilde{E}}{\partial x}\right|_{x=x_0} \tag{33}$$

hence, we can write

$$\frac{\mathrm{d}E}{\mathrm{d}x} = \langle 0|\frac{\partial\hat{H}}{\partial x}|0\rangle + \langle 0|\left(\frac{\partial\hat{W}_{\mathrm{N}}}{\partial x}\hat{T}^{(1)}_{2}\right)_{c}|0\rangle + \langle 0|\left\{\hat{\Lambda}^{(1)}_{2}\left(\frac{\partial\hat{f}^{d}_{\mathrm{N}}}{\partial x}\hat{T}^{(1)}_{2} + \frac{\partial\hat{W}_{\mathrm{N}}}{\partial x}\right)_{c}\right\}_{c}|0\rangle \tag{34}$$

when we insert the explicit equations for $\tilde{h}^{x}_{pq}$ and $\tilde{g}^{x}_{pqrs}$ into eq 34 and define particle density matrices (PDMs), the gradient expression can be cast into the following form, as shown in our recent study[46]

$$\frac{\mathrm{d}E}{\mathrm{d}x} = \sum_{p,q}\gamma_{pq}h^{x}_{pq} - \sum_{p,q}F_{pq}S^{x}_{pq} + \sum_{\mathrm{Q}}^{N_{\mathrm{aux}}}\sum_{pq}\tilde{\Gamma}^{\mathrm{Q}}_{pq}(\mathrm{Q}|pq)^{x} - \sum_{P,\mathrm{Q}}^{N_{\mathrm{aux}}}\Gamma_{P\mathrm{Q}}\mathbf{J}^{x}_{P\mathrm{Q}} \tag{35}$$

where F_{pq} is the generalized-Fock matrix (GFM),[3,11−14] and one-particle density matrix (OPDM) can be written as[46]

$$\gamma_{pq} = \langle 0|\hat{p}^{\dagger}\hat{q}|0\rangle + \langle 0|\{\hat{\Lambda}^{(1)}_{2}(\{\hat{p}^{\dagger}\hat{q}\}^{d}\hat{T}^{(1)}_{2})_{c}\}_{c}|0\rangle \tag{36}$$

similarly, two-particle density matrix (TPDM) are defined as[46]

$$\Gamma^{\mathrm{Q}}_{pq} = \sum_{r,s} b^{\mathrm{Q}}_{rs}\langle 0|\hat{p}^{\dagger}\hat{q}^{\dagger}\hat{s}\hat{r}|0\rangle + \sum_{r,s} b^{\mathrm{Q}}_{rs}\langle 0|(\{\hat{p}^{\dagger}\hat{q}^{\dagger}\hat{s}\hat{r}\}\hat{T}^{(1)}_{2})_{c}|0\rangle + \sum_{r,s} b^{\mathrm{Q}}_{rs}\langle 0|(\hat{\Lambda}^{(1)}_{2}\{\hat{p}^{\dagger}\hat{q}^{\dagger}\hat{s}\hat{r}\})_{c}|0\rangle \tag{37}$$

$$\tilde{\Gamma}^{\mathrm{Q}}_{pq} = \sum_{P}^{N_{\mathrm{aux}}}\Gamma^{P}_{pq}[\mathbf{J}^{-1/2}]_{P\mathrm{Q}} \tag{38}$$

$$\Gamma_{P\mathrm{Q}} = \frac{1}{2}\sum_{p,q} c^{P}_{pq}\tilde{\Gamma}^{\mathrm{Q}}_{pq} = \frac{1}{2}\sum_{p,q}\tilde{\Gamma}^{P}_{pq}c^{\mathrm{Q}}_{pq} \tag{39}$$

and

$$c^{\mathrm{Q}}_{pq} = \sum_{P}^{N_{\mathrm{aux}}} b^{P}_{pq}[\mathbf{J}^{-1/2}]_{P\mathrm{Q}} \tag{40}$$

note that these are the "unrelaxed" density matrices; because the orbitals are optimized, we do not need the additional orbital response contributions that would normally present. Explicit equations for PDMs are provided in the next section.

The gradient is evaluated in the usual way by back-transforming the PDMs and GFM into the AO basis and contracting against the appropriate AO derivative integrals[46,56,57]

$$F_{\mu\nu} = \sum_{pq} C_{\mu p}C_{\nu q}F_{pq} \tag{41}$$

$$\gamma_{\mu\nu} = \sum_{pq} C_{\mu p}C_{\nu q}\gamma_{pq} \tag{42}$$

$$\Gamma^{\mathrm{Q}}_{\mu\nu} = \sum_{pq} C_{\mu p}C_{\nu q}\tilde{\Gamma}^{\mathrm{Q}}_{pq} \tag{43}$$

where $F_{\mu\nu}$, $\gamma_{\mu\nu}$, and $\Gamma^{\mathrm{Q}}_{\mu\nu}$ are the AO basis GFM, OPDM, and 3-index TPDM, respectively. The 2-index TPDM can be written as

dx.doi.org/10.1021/ct500634s | J. Chem. Theory Comput. 2014, 10, 4389−4399

$$\Gamma_{PQ} = \frac{1}{2}\sum_{p,q} c_{pq}^{P}\tilde{\Gamma}_{pq}^{Q} = \frac{1}{2}\sum_{\mu\nu} c_{\mu\nu}^{P}\Gamma_{\mu\nu}^{Q} \tag{44}$$

$$c_{\mu\nu}^{Q} = \sum_{P}^{N_{aux}} b_{\mu\nu}^{P}[\mathbf{J}^{-1/2}]_{PQ} \tag{45}$$

hence, the final gradient equation in the AO basis can be written as follows

$$\frac{dE}{dx} = \sum_{\mu\nu}\gamma_{\mu\nu}h_{\mu\nu}^{x} - \sum_{\mu\nu}F_{\mu\nu}S_{\mu\nu}^{x} + \sum_{Q}^{N_{aux}}\sum_{\mu\nu}\Gamma_{\mu\nu}^{Q}(Q|\mu\nu)^{x} - \sum_{P,Q}^{N_{aux}}\Gamma_{PQ}\mathbf{J}_{PQ}^{x} \tag{46}$$

2.5. Response Density Matrices. At first, the one-particle density matrix (OPDM) can be decomposed as follows

$$\gamma_{pq} = \gamma_{pq}^{ref} + \gamma_{pq}^{corr} \tag{47}$$

where γ_{pq}^{ref} and γ_{pq}^{corr} are the reference and correlation contributions to OPDM. The reference OPDM is given by

$$\gamma_{ij}^{ref} = \delta_{ij} \tag{48}$$

where δ_{ij} denotes the Kronecker δ. The unique nonzero blocks of the correlation OPDM can be written as

$$\gamma_{ij}^{corr} = -\frac{1}{2}\sum_{m}^{occ}\sum_{e,f}^{vir} t_{im}^{ef(1)}\lambda_{ef}^{jm(1)} \tag{49}$$

$$\gamma_{ab}^{corr} = -\frac{1}{2}\sum_{m,n}^{occ}\sum_{f}^{vir} t_{mn}^{bf(1)}\lambda_{af}^{mn(1)} \tag{50}$$

where

$$\lambda_{ab}^{ij(1)} = t_{ij}^{ab(1)} \tag{51}$$

Similar to the OPDM case, the two-particle density matrix (TPDM) can be decomposed as follows[14]

$$\Gamma_{pq}^{Q} = \Gamma_{pq}^{Q(ref)} + \Gamma_{pq}^{Q(corr)} + \Gamma_{pq}^{Q(sep)} \tag{52}$$

where $\Gamma_{pq}^{Q(ref)}$ and $\Gamma_{pq}^{Q(corr)}$ are the reference and correlation contributions to TPDM, and $\Gamma_{pq}^{Q(sep)}$ is the separable part of TPDM. The reference TPDM is given by

$$\Gamma_{ij}^{Q(ref)} = \delta_{ij}J_{Q} - b_{ij}^{Q} \tag{53}$$

where b_{ij}^{Q} is evaluated using the reference auxiliary (DF-REF) basis, the JK-FIT basis set,[31] and J_Q is defined as

$$J_{Q} = \sum_{m}^{occ} b_{mm}^{Q} \tag{54}$$

The unique nonzero blocks of the separable TPDMs can be written as[14]

$$\Gamma_{ij}^{Q(sep)} = \delta_{ij}(\gamma_{Q} + \tilde{\gamma}_{Q}) + \gamma_{ij}^{corr}J_{Q} - \sum_{m}^{occ}\gamma_{mj}^{corr}b_{mi}^{Q} - \sum_{m}^{occ}\gamma_{im}^{corr}b_{jm}^{Q} \tag{55}$$

$$\Gamma_{ia}^{Q(sep)} = -\sum_{e}^{vir}\gamma_{ea}^{corr}b_{ie}^{Q} \tag{56}$$

$$\Gamma_{ab}^{Q(sep)} = \gamma_{ab}^{corr}J_{Q} \tag{57}$$

where b_{pq}^{Q} is again evaluated in the DF-REF basis, and intermediates are given by

$$\gamma_{Q} = \sum_{m,n}^{occ}\gamma_{mn}^{corr}b_{mn}^{Q} \tag{58}$$

$$\tilde{\gamma}_{Q} = \sum_{e,f}^{vir}\gamma_{ef}^{corr}b_{ef}^{Q} \tag{59}$$

Finally, the unique nonzero blocks of the correlation TPDM can be expressed as[14]

$$\Gamma_{ia}^{Q(corr)} = \sum_{m}^{occ}\sum_{e}^{vir} t_{im}^{ae(1)}b_{me}^{Q} \tag{60}$$

where b_{me}^{Q} is evaluated using the correlation auxiliary (DF-MP2) basis, the RI basis set.[58]

2.6. Generalized-Fock Matrix. As in the case of PDMs, it is possible to separate GFM into reference, correlation, and separable parts:[14]

$$F_{pq} = F_{pq}^{ref} + F_{pq}^{corr} + F_{pq}^{sep} \tag{61}$$

More explicitly, we can write

$$F_{pq}^{ref} = \sum_{r} h_{pr}\gamma_{rq}^{ref} + \sum_{Q}^{N_{aux}}\sum_{r}\Gamma_{qr}^{Q(ref)}b_{pr}^{Q} \tag{62}$$

$$F_{pq}^{corr} = \sum_{r} h_{pr}\gamma_{rq}^{corr} + \sum_{Q}^{N_{aux}}\sum_{r}\Gamma_{qr}^{Q(corr)}b_{pr}^{Q} \tag{63}$$

$$F_{pq}^{sep} = \sum_{Q}^{N_{aux}}\sum_{r}\Gamma_{qr}^{Q(sep)}b_{pr}^{Q} \tag{64}$$

For F_{pq}^{ref} and F_{pq}^{sep} one should use the DF-REF basis integrals, while for F_{pq}^{corr} the DF-MP2 basis integrals should be employed. For F_{pq}^{ref} we have the following equations

$$F_{ij}^{ref} = f_{ij} \tag{65}$$

$$F_{ai}^{ref} = f_{ai} \tag{66}$$

$$F_{ia}^{ref} = 0 \tag{67}$$

$$F_{ab}^{ref} = 0 \tag{68}$$

2.7. Evaluation of $\langle S^2\rangle$ for Unrestricted DF-OMP2. To better appreciate the success of the DF-OMP2 method compared to the standard MP2, we evaluate $\langle S^2\rangle$ for the unrestricted DF-OMP2 wave function. The computation of the $\langle S^2\rangle$ value will allow us to analyze the success of DF-OMP2 in the case of spin-contamination problems. We present two approaches to compute the $\langle S^2\rangle$ value.

2.7.1. Response Theory Approach. For the response theory approach, we follow the formulation of Schlegel,[59] which is implemented for the OO-RI-MP2 method by Kossmann and

Neese.[22] In this approach, the Hamiltonian operator is augmented by a $\lambda\hat{S}^2$ term

$$\hat{H} = \hat{H}_0 + \lambda\hat{S}^2 \tag{69}$$

where λ is the perturbation parameter. Then, $\langle S^2\rangle$ can be written as

$$\langle S^2\rangle = \left.\frac{dE(\lambda)}{d\lambda}\right|_{\lambda=0} \tag{70}$$

For a general UMPn method, one can write

$$\langle S^2\rangle = \sum_{i=0}^{n-1} \langle S^2\rangle^{(i)} \tag{71}$$

and

$$\langle S^2\rangle^{(i)} = \left.\frac{dE^{(i+1)}(\lambda)}{d\lambda}\right|_{\lambda=0} \tag{72}$$

Up to second-order (MP2), we have

$$\langle S^2\rangle^{(0)} = \langle 0|\hat{S}^2|0\rangle \tag{73}$$

$$\langle S^2\rangle^{(1)} = 2\langle 0|\hat{S}^2|\Psi^{(1)}\rangle \tag{74}$$

$$\langle S^2\rangle_{MP2} = \langle S^2\rangle^{(0)} + \langle S^2\rangle^{(1)} \tag{75}$$

where $|\Psi^{(1)}\rangle$ is the first-order wave function correction. When we evaluate $\langle S^2\rangle^{(0)}$, we obtain

$$\langle S^2\rangle^{(0)} = \frac{1}{4}(N^\alpha - N^\beta)^2 + \frac{1}{2}(N^\alpha + N^\beta) - \sum_{Ij}^{occ} S_{Ij}S_{jI} \tag{76}$$

where N^α and N^β is the number of α and β electrons, respectively, upper and lower case letters refer to α and β spin orbitals, and **S** is the overlap matrix. The explicit form of $\langle S^2\rangle^{(1)}$ can be written as follows

$$\langle S^2\rangle^{(1)} = -\frac{1}{2}\sum_{Ij}^{occ}\sum_{Ab}^{vir} S_{Ib}S_{jA}t_{Ij}^{Ab(1)} \tag{77}$$

2.7.2. Projective Approach. In the projective approach, we compute $\langle S^2\rangle$ as a projection as in the case of the energy.[60] For a general projective method, if the energy is computed as

$$E = \langle\Phi|\hat{H}|\Psi\rangle \tag{78}$$

then, $\langle S^2\rangle$ can be evaluated as follows

$$\langle S^2\rangle = \langle\Phi|\hat{S}^2|\Psi\rangle \tag{79}$$

Hence, for the unrestricted DF-OMP2, we obtain the following equation

$$\langle S^2\rangle = \frac{1}{4}(N^\alpha - N^\beta)^2 + \frac{1}{2}(N^\alpha + N^\beta) - \sum_{Ij}^{occ} S_{Ij}S_{jI} - \sum_{Ij}^{occ}\sum_{Ab}^{vir} S_{Ib}S_{jA}t_{Ij}^{Ab(1)} \tag{80}$$

Note that there is a factor of $^1/_2$ in front of the last term of eq 80 in the response theory approach, which leads a minor difference between two approaches.

3. RESULTS AND DISCUSSION

Results from the DF-OMP2 and OO-RI-MP2 methods were obtained for a set of alkanes,[14] conjugated dines,[14] and the S22 database[61] for comparison of the computational cost for single point analytic gradient computations. For alkanes and conjugated dienes, Dunning's correlation-consistent polarized valence triple-ζ basis set (cc-pVTZ) was used, whereas for the S22 database Dunning's augmented correlation-consistent polarized valence double-ζ basis set (aug-cc-pVDZ) was employed without the frozen core approximation.[62,63] For the cc-pVTZ and aug-cc-pVDZ primary basis sets, cc-pVTZ-JKFIT[31] and cc-pVTZ-RI;[58] and aug-cc-pVDZ-JKFIT[31] and aug-cc-pVDZ-RI[58] auxiliary basis set pairs were used for reference and correlation energies, respectively.

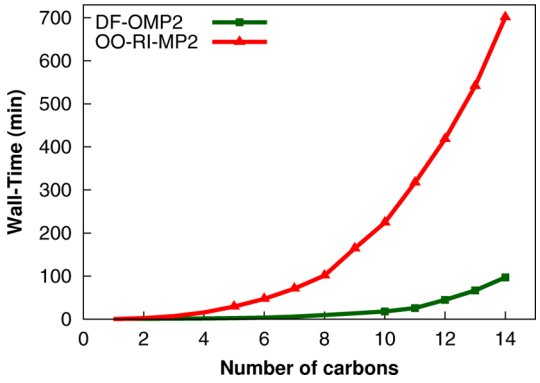

Figure 1. Wall-time (in min) for computations of single-point analytic gradients for the C_nH_{2n+2} (n = 1−14) set from the DF-OMP2 and OO-RI-MP2 methods with the cc-pvtz basis set. For the largest member, the number of basis functions is 840. All computation were performed with an 10^{-8} energy convergence tolerance on a single node (nproc = 12) Intel Core i7-4930K CPU @ 3.40 GHz computer (memory ~64 GB).

Moreover, aromatic bond dissociation energies (ABDE), where the standard MP2 has difficulties, were studied to investigate the performance of MP2, DF-OMP2, OO-RI-MP2, coupled-cluster singles and doubles (CCSD),[64] and coupled-cluster singles and doubles with perturbative triples [CCSD-(T)].[65,66] For the ABDE test set the cc-pVTZ basis set was used without the frozen core approximation. Optimized geometries (at B3LYP/6-311G(d,p) level[67,68]) of the ABDE set members were reported in the Supporting Information, some of them were taken from our previous studies.[69−75] The cc-pVTZ-JKFIT[31] and cc-pVTZ-RI[58] auxiliary basis sets were employed as fitting basis sets. For open-shell radicals, the unrestricted orbitals were employed, and no mixing of α and β spin orbitals was allowed.

Additionally, equilibrium geometries of several molecules were considered to investigate the performance of the MP2, DF-OMP2, OO-RI-MP2, CCSD, and CCSD(T) methods. For geometry optimizations, Dunning's correlation-consistent polarized valence quadruple-ζ basis set (cc-pVQZ) was used without the frozen core approximation.[62,63] The cc-pVQZ-JKFIT[31] and cc-pVQZ-RI[58] basis sets were employed as auxiliary basis sets. The MP2, DF-MP2, DF-OMP2, CCSD, and CCSD(T) computations were performed with the PSI4 package,[40] while the OO-RI-MP2 computations were carried out with the ORCA3.0.0 program.[20,22,76]

dx.doi.org/10.1021/ct500634s | J. Chem. Theory Comput. 2014, 10, 4389−4399

Table 1. Wall-Time for the Evaluation of Gradient Terms for Single-Point Analytic Gradient Computations for the C_nH_{2n+2} (n = 1−14) Set from the DF-OMP2 and OO-RI-MP2 Methods with the cc-pvtz Basis Set[a]

	separable grad (min)		3-index grad (s)[b]		metric grad (s)[c]	
alkane	DF-OMP2	OO-RI-MP2	DF-OMP2	OO-RI-MP2	DF-OMP2	OO-RI-MP2
CH_4	0.02	0.05	0.00	0.29	0.00	0.01
C_2H_6	0.00	0.32	0.00	1.53	0.00	0.04
C_3H_8	0.02	1.00	1.00	4.37	0.00	0.08
C_4H_{10}	0.03	2.10	1.00	8.96	0.00	0.14
C_5H_{12}	0.03	3.70	2.00	15.63	0.00	0.21
C_6H_{14}	0.05	5.73	4.00	23.92	1.00	0.31
C_7H_{16}	0.08	8.10	5.00	34.22	0.00	0.43
C_8H_{18}	0.13	10.75	7.00	46.20	0.00	0.57
C_9H_{20}	0.17	14.64	10.00	61.44	0.00	0.78
$C_{10}H_{22}$	0.23	18.53	13.00	77.74	0.00	0.93
$C_{11}H_{24}$	0.28	22.82	18.00	96.36	0.00	1.14
$C_{12}H_{26}$	0.38	27.63	22.00	115.86	0.00	1.37
$C_{13}H_{28}$	0.45	32.76	27.00	138.77	1.00	1.65
$C_{14}H_{30}$	0.58	38.34	35.00	164.33	0.00	1.96

[a]For the largest member, the number of basis functions is 840. All computation were performed on a single node (nproc = 12) Intel Core i7-4930K CPU @ 3.40 GHz computer (memory ∼64 GB). [b]The correlation part of the third term of eq 46. [c]The correlation part of the fourth term of eq 46.

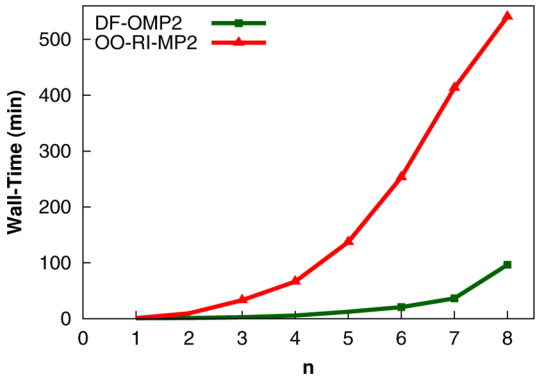

Figure 2. Wall-time (in min) for computations of single-point analytic gradients for the conjugated dienes ($C_{2n}H_{2n+2}$) from the DF-OMP2 and OO-RI-MP2 methods with the cc-pvtz basis set. For the largest member, the number of basis functions is 732. All computation were performed with an 10^{-8} energy convergence tolerance on a single node (nproc = 12) Intel Core i7-4930K CPU @ 3.40 GHz computer (memory ∼64 GB).

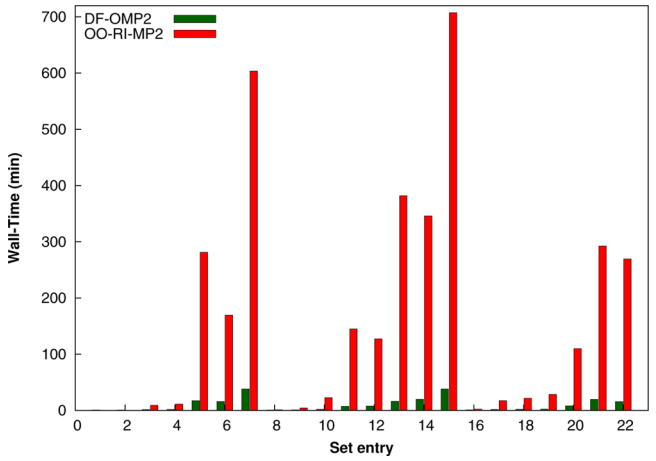

Figure 3. Wall-time (in min) for computations of single-point analytic gradients for dimers of the S22 database from the DF-OMP2 and OO-RI-MP2 methods with the aug-cc-pVDZ basis set. For the largest member, the number of basis functions is 536. All computation were performed with an 10^{-8} energy convergence tolerance on a single node (nproc = 12) Intel Core i7-4930K CPU @ 3.40 GHz computer (memory ∼64 GB).

In all computations, the same energy and orbital convergence criteria were used for OO-RI-MP2 and DF-OMP2, and all computations were performed on the same computer with

Table 2. Wall-Time for the Evaluation of Gradient Terms for Single-Point Analytic Gradient Computations for the Conjugated Dienes ($C_{2n}H_{2n+2}$) from the DF-OMP2 and OO-RI-MP2 Methods with the cc-pvtz Basis Set[a]

	separable grad (min)		3-index grad (s)[b]		metric grad (s)[c]	
diene	DF-OMP2	OO-RI-MP2	DF-OMP2	OO-RI-MP2	DF-OMP2	OO-RI-MP2
C_2H_4	0.00	0.16	0.00	0.88	0.00	0.02
C_4H_6	0.00	1.08	0.00	4.95	1.00	0.09
C_6H_8	0.03	2.96	2.00	13.44	1.00	0.20
C_8H_{10}	0.07	5.84	4.00	25.85	1.00	0.36
$C_{10}H_{12}$	0.12	9.52	7.00	41.41	0.00	0.58
$C_{12}H_{14}$	0.18	14.13	11.00	63.16	0.00	0.86
$C_{14}H_{16}$	0.30	19.68	17.00	87.53	0.00	1.20
$C_{16}H_{18}$	0.45	26.55	25.00	118.44	0.00	1.61

[a]For the largest member, the number of basis functions is 732. All computation were performed on a single node (nproc = 12) Intel Core i7-4930K CPU @ 3.40 GHz computer (memory ∼64 GB). [b]The correlation part of the third term of eq 46. [c]The correlation part of the fourth term of eq 46.

dx.doi.org/10.1021/ct500634s | J. Chem. Theory Comput. 2014, 10, 4389−4399

Table 3. Wall-Time for the Evaluation of Gradient Terms for Single-Point Analytic Gradient Computations for Dimers of the S22 Database from the DF-OMP2 and OO-RI-MP2 Methods with the aug-cc-pVDZ Basis Set[a]

	separable grad (min)		3-index grad (s)[b]		metric grad (s)[c]	
set entry	DF-OMP2	OO-RI-MP2	DF-OMP2	OO-RI-MP2	DF-OMP2	OO-RI-MP2
1	0.02	0.08	0.00	0.40	0.00	0.02
2	0.00	0.04	0.00	0.25	0.00	0.01
3	0.02	0.81	1.00	3.16	0.00	0.08
4	0.02	1.10	0.00	3.96	0.00	0.09
5	0.15	17.00	7.00	45.18	0.00	0.63
6	0.15	16.35	7.00	39.69	0.00	0.63
7	0.28	33.65	13.00	78.64	0.00	0.99
8	0.02	0.16	0.00	0.62	0.00	0.02
9	0.02	0.58	1.00	2.04	0.00	0.05
10	0.03	3.18	1.00	8.45	0.00	0.15
11	0.10	15.28	5.00	31.44	0.00	0.43
12	0.07	11.06	4.00	25.38	0.00	0.36
13	0.15	24.37	8.00	53.17	0.00	0.64
14	0.18	31.23	9.00	55.85	0.00	0.67
15	0.27	50.64	13.00	91.35	1.00	0.99
16	0.00	0.35	0.00	1.51	0.00	0.05
17	0.03	2.50	2.00	7.19	0.00	0.14
18	0.02	2.81	1.00	7.69	0.00	0.14
19	0.03	3.07	2.00	8.87	0.00	0.16
20	0.10	12.98	5.00	29.79	0.00	0.42
21	0.20	25.77	9.00	52.57	0.00	0.66
22	0.13	18.35	6.00	42.21	1.00	0.57

[a]For the largest member, the number of basis functions is 536. All computation were performed on a single node (nproc = 12) Intel Core i7-4930K CPU @ 3.40 GHz computer (memory ~64 GB). [b]The correlation part of the third term of eq 46. [c]The correlation part of the fourth term of eq 46.

Table 4. Aromatic Bond Dissociation Energies (in kcal mol^{-1}) at the cc-pVTZ MP2, DF-OMP2, OO-RI-OMP2, CCSD, and CCSD(T) Levels

	radical	MP2	DF-OMP2	OO-RI-MP2	CCSD	CCSD(T)
1	phenyl	143.7	118.3	118.3	120.8	121.5
2	4-methylphenyl	144.7	118.7	118.7	121.1	121.9
3	benzyl	120.1	96.7	96.7	96.9	98.6
4	3,4-dimethylphenyl	144.8	118.4	118.4	120.9	121.7
5	2-methylbenzyl	120.6	96.6	96.6	96.7	98.5
6	2,6-dimethylphenyl	144.4	118.1	118.1	120.5	121.3
7	3,5-dimethylphenyl	145.0	118.5	118.5	121.0	121.8
8	3-methylbenzyl	120.3	96.6	96.6	96.7	98.5
9	4-methylbenzyl	120.4	96.3	96.3	96.5	98.3
10	2-aminophenyl	143.4	119.0	119.0	121.2	122.0
11	3-aminophenyl	141.2	118.1	118.1	120.3	121.0
12	4-aminophenyl	144.3	119.6	119.6	121.8	122.5
13	anilino	124.2	99.3	99.3	97.4	99.2
14	4-hydroxyphenyl	144.7	119.7	119.7	121.9	122.6
15	phenoxy	122.3	95.1	95.2	94.1	96.2

same number of processors and the same amount of memory. All computation were performed with the 10^{-8} au energy and 10^{-6} au orbital gradient convergence tolerance. For DF-OMP2 we did not use any integral cutoff limit, all integrals were computed, while for OO-RI-MP2 the default value of 2.5×10^{-11} was used. For the DF-OMP2 method, the DF integrals are computed and written to the disk. Whenever DF integrals are needed, they are stored in the core memory, and when the related computation is over, the allocated memory is released. The same disk/memory hybrid algorithm is also used for PDMs. In the evaluation of analytic gradients of DF-OMP2, integral derivatives are computed on the fly and contracted with PDMs.

3.1. Efficiency of DF-OMP2 Gradient. In order to assess the efficiency of the DF-OMP2 analytic gradients, we start with a set of alkanes.[14] The computational (wall) time for single point analytic gradient computations from the DF-OMP2 and OO-RI-MP2 methods are presented graphically in Figure 1. The DF-OMP2 method substantially reduces the computational cost compared to OO-RI-MP2; there are up to 13-fold reductions in the computational time compared to OO-RI-MP2. On average, the cost of DF-OMP2 analytic gradients is 9.1 times lower than that of OO-RI-MP2. To further analyze the efficiency of DF-OMP2 gradients, the relative costs for the computing the gradient terms are reported in Table 1. Especially for the computation of the separable gradient

dx.doi.org/10.1021/ct500634s | J. Chem. Theory Comput. 2014, 10, 4389−4399

Table 5. $\langle S^2 \rangle$ Values (in au) for the Aromatic Radicals from the UHF and DF-OMP2 Wave Functions[a]

radical	$\langle S^2 \rangle_{UHF}$	$\langle S^2 \rangle_{REF}$	$\langle S^2 \rangle_{RESP}$	$\langle S^2 \rangle_{PROJ}$
phenyl	1.3567	0.7574	0.7558	0.7542
4-methylphenyl	1.3688	0.7551	0.7525	0.7500
benzyl	1.3430	0.7636	0.7586	0.7535
3,4-dimethylphenyl	1.3674	0.7549	0.7523	0.7498
2-methylbenzyl	1.3442	0.7628	0.7578	0.7529
2,6-dimethylphenyl	1.3649	0.7557	0.7529	0.7501
3,5-dimethylphenyl	1.3713	0.7546	0.7522	0.7498
3-methylbenzyl	1.3455	0.7632	0.7582	0.7532
4-methylbenzyl	1.3469	0.7626	0.7577	0.7528
2-aminophenyl	1.3329	0.7544	0.7522	0.7500
3-aminophenyl	1.3046	0.7567	0.7533	0.7500
4-aminophenyl	1.3508	0.7533	0.7514	0.7495
anilino	1.3646	0.7613	0.7558	0.7503
4-hydroxyphenyl	1.3528	0.7534	0.7514	0.7495
phenoxy	1.3442	0.7586	0.7539	0.7492

[a]For DF-OMP2 wave function both response ($\langle S^2 \rangle_{RESP}$) and projected ($\langle S^2 \rangle_{PROJ}$) values are computed. Additionally, the $\langle S^2 \rangle$ value for the reference wave function of DF-OMP2 is reported ($\langle S^2 \rangle_{REF}$). For aromatic radicals considered, the theoretical value of $\langle S^2 \rangle$ is 0.75.

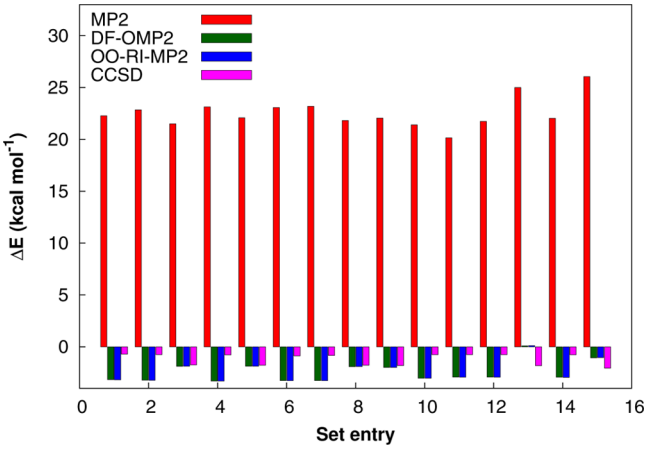

Figure 4. Errors in aromatic bond dissociation energies for the MP2, DF-OMP2, OO-RI-MP2, and CCSD methods with respect to CCSD(T) (the cc-pVTZ basis set was employed).

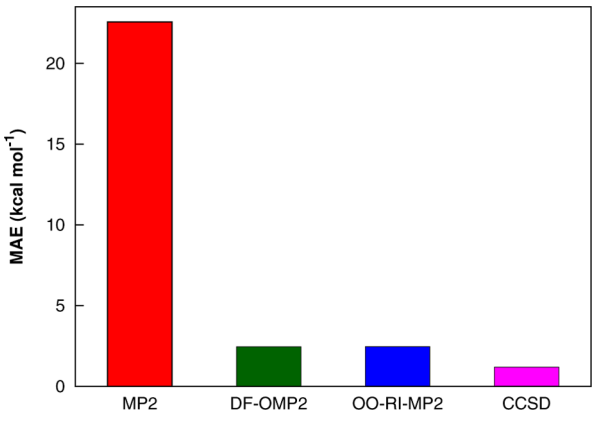

Figure 5. Mean absolute errors (in kcal mol^{-1}) in aromatic bond dissociation energies for the MP2, DF-OMP2, OO-RI-MP2, and CCSD methods with respect to CCSD(T) (the cc-pVTZ basis set was employed).

(including the reference contribution), which is the most time-consuming gradient term, there are dramatic improvements on OO-RI-MP2. For example for the largest member ($C_{14}H_{30}$) the cost of the separable gradient is 38.3 min for OO-RI-MP2, while it is only 0.6 min for DF-OMP2. The dramatic reduction in the cost of the computation of the separable gradient is arising from the usage of 3-index integrals instead of 4-index integrals, which are used in the case of OO-RI-MP2.

As the second step of our assessment, we consider a set of conjugated dienes.[14] For the considered conjugated dienes, the computational time for single point analytic gradients of the DF-OMP2 and OO-RI-MP2 methods are presented graphically in Figure 2. The DF-OMP2 method significantly decreases the cost of analytic gradients compared to OO-RI-MP2, there are up to 13-fold reductions in the computational time compared to OO-RI-MP2. On average, the cost of DF-OMP2 is 9.2 times lower than that of OO-RI-MP2. To further investigate the efficiency of DF-OMP2 gradients, the relative costs for the computing the gradient terms are reported in Table 2. Especially for the computation of the separable gradient (including the reference contribution), which is the most time-consuming gradient term, there are remarkable improvements on OO-RI-MP2. For example, for the largest member ($C_{16}H_{18}$), the cost of the separable gradient is 26.6 min for OO-RI-MP2, while it is only 0.5 min for DF-OMP2. The remarkable reduction in the cost of the computation of the separable gradient is arising from the usage of 3-index integrals instead of 4-index integrals, which are used in the case of OO-RI-MP2.

As the final step of our investigation, we turn our attention to dimers of the S22 database.[61] For dimers of the S22 database, the computational time for single point analytic gradients of the DF-OMP2 and OO-RI-MP2 methods are presented graphically in Figure 3. The DF-OMP2 method again substantially reduces the computational cost compared to OO-RI-MP2, there are up to 24-fold reductions in the cost compared to OO-RI-MP2. On average, the cost of DF-OMP2 analytic gradients is 11.3 times lower than that of OO-RI-MP2. The relative costs for the computing the gradient terms are reported in Table 3. Especially for the computation of the separable gradient (including the reference contribution), which is the most time-consuming gradient term, there are great improvements on OO-RI-MP2. For example for the largest member (stacked adenine···thymine complex) the cost of the separable gradient is 50.6 min for OO-RI-MP2, while it is only 0.3 min for DF-OMP2. The significant reduction in the cost of the computation of the separable gradient is again attributed to the usage of 3-index integrals instead of 4-index integrals, which are used in the case of OO-RI-MP2.

3.2. Aromatic Bond Dissociation Energies. In the previous section, the efficiency of DF-OMP2 analytic gradients has been demonstrated. Now, we assess the performance of DF-OMP2 for aromatic bond dissociation energies, where the standard MP2 dramatically fails due to high spin-contamination problem. The following general reaction is employed in the evaluation of the ABDE for an aromatic radical.

$$Ar - H \rightarrow Ar\bullet + \bullet H$$

For the considered set, the ABDE values (in kcal mol^{-1}) at the cc-pVTZ MP2, DF-OMP2, OO-RI-MP2, CCSD, and CCSD(T) levels are reported in Table 4, whereas $\langle S^2 \rangle$ values for the aromatic radicals considered are presented in Table 5. Errors with respect to CCSD(T)/cc-pVTZ are presented

Table 6. Bond Lengths (in Å) of Molecules Considered at the cc-pVQZ MP2, DF-OMP2, OO-RI-OMP2, CCSD, and CCSD(T) Levels, the Experimental Values, Mean Absolute Errors (MAE), and Standard Deviation of Errors (STD)

molecule	bond	MP2	DF-OMP2	OO-RI-MP2	CCSD	CCSD(T)	expt.[a]
H_2O	R_{OH}	0.956	0.958	0.958	0.955	0.958	0.958
HNC	R_{NH}	0.994	0.995	0.995	0.994	0.996	0.994
HNC	R_{CN}	1.170	1.177	1.177	1.165	1.172	1.169
NH_3	R_{NH}	1.008	1.009	1.009	1.010	1.012	1.012
NH_4^+	R_{NH}	1.018	1.019	1.019	1.020	1.021	1.021
C_2H_2	R_{CH}	1.059	1.059	1.059	1.062	1.062	1.062
C_2H_2	R_{CC}	1.206	1.210	1.211	1.204	1.204	1.203
FCCH	R_{CH}	1.057	1.057	1.057	1.059	1.061	1.063
FCCH	R_{CC}	1.199	1.204	1.204	1.193	1.210	1.206
FCCH	R_{CF}	1.274	1.277	1.277	1.275	1.299	1.281
HCN	R_{CH}	1.062	1.063	1.063	1.065	1.067	1.065
HCN	R_{CN}	1.161	1.167	1.167	1.149	1.156	1.153
CH_4	R_{CH}	1.082	1.082	1.082	1.086	1.088	1.086
CO_2	R_{CO}	1.164	1.173	1.173	1.155	1.163	1.160
H_2CO	R_{CH}	1.097	1.098	1.098	1.100	1.102	1.099
H_2CO	R_{CO}	1.206	1.212	1.212	1.200	1.207	1.203
	MAE	0.004	0.005	0.005	0.003	0.003	
	STD	0.001	0.002	0.002	0.001	0.001	

[a]Data from Thomas et al.[77] and references therein.

graphically in Figure 4, while the MAE values are depicted in Figure 5.

The MAE values are 22.6 (MP2), 2.5 (DF-OMP2), 2.5 (OO-RI-MP2), and 1.2 (CCSD) kcal mol^{-1}, indicating a reduction in MP2 errors by more than a factor of 9 when optimized orbitals are employed. Of course, the MAE of CCSD (1.2 kcal mol^{-1}) provides significant further improvement over DF-OMP2 but at a greatly increased computational cost [scaling formally as $O(N^6)$ for CCSD compared to $O(N^5)$ for DF-OMP2]. Overall, it appears that the DF-OMP2 method can be reliably used for aromatic bond dissociation energies when more sophisticated methods such as CCSD or CCSD(T) are too computationally costly.

Failures of the MP2 method can be attributed to spin-contamination in the reference UHF wave function. As it is shown in Table 5, for aromatic radicals $\langle S^2 \rangle$ values of the reference UHF wave function is significantly contaminated; hence, UHF wave functions have considerably larger $\langle S^2 \rangle$ values than the theoretical value of 0.75. On the other hand, the $\langle S^2 \rangle$ values of the DF-OMP2 wave function are quite close to 0.75, indicating negligible spin-contamination. As in the case of the entire DF-OMP2 wave function, the DF-OMP2 reference wave function has also a quite negligible spin-contamination, indicating that the contamination of the UHF reference is arising from the lack of correlation effects in the UHF wave function.

3.3. Geometries. Finally, we consider several molecules to assess the performance of DF-OMP2 for equilibrium geometries. Table 6 reports bond lengths of molecules considered.[77] The MAE values are 0.004 (MP2), 0.005 (DF-OMP2), 0.005 (OO-RI-MP2), 0.003 (CCSD), and 0.003 [CCSD(T)] Å. Further, the standard deviation of errors (STDs) are 0.001 (MP2), 0.002 (DF-OMP2), 0.002 (OO-RI-MP2), 0.001 (CCSD), and 0.001 [CCSD(T)] Å. Hence, the performance of the MP2, DF-OMP2, and OO-RI-MP2 methods are essentially the same, while that of CCSD and CCSD(T) are somewhat better, as expected.

4. CONCLUSIONS

An efficient implementation of analytic energy gradients and spin multiplicities for the density-fitted orbital-optimized MP2 method (DF-OMP2) has been presented. The computational time of the DF-OMP2 single point analytic gradients have been compared with that of OO-RI-MP2.[20] Our results demonstrate that the DF-OMP2 method provides significantly lower costs than OO-RI-MP2 for analytic gradient computations. On average, the cost of DF-OMP2 analytic gradients is 9−11 times lower than that of OO-RI-MP2.

For all considered test sets, the DF-OMP2 substantially accelerates the OO-RI-MP2 method for analytic gradient computations. The reason why the DF-OMP2 method provides significantly lower costs than OO-RI-MP2 is that in the OO-RI-MP2 method, the DF approximation was applied only to the correlation energy, while in DF-OMP2 we use the DF approach to reference energy as well. In other words, we completely avoid the storage or the generation of the 4-index ERIs, and 3-index TEI tensors are employed instead. Further, as in case of integrals, our gradient equation is completely avoid the generation or the storage of the 4-index TPDMs, instead, we use 2- and 3-index TPDMs. Hence, the I/O bottleneck of a gradient computation is significantly overcome in many cases. Therefore, the cost GFM, PDMs, back transformation of TPDMs, and integral derivatives are substantially reduced when the DF approach is used for the entire energy expression. This is not the case for the OO-RI-MP2 method, where one need to consider the conventional integrals for the reference energy and its derivatives. However, the implementation of OO-RI-MP2 in ORCA may benefit from some coding improvement (computation and contraction of integrals on-the-fly, rather than storing them on disk), which may help to somewhat reduce the difference in timing with DF-OMP2.

Moreover, for aromatic bond dissociation energies (ABDEs), the DF-OMP2 method (MAE = 2.5 kcal mol^{-1}) exhibits a dramatically better performance than MP2 (MAE = 22.6 kcal mol^{-1}). This result demonstrate that the DF-OMP2 method is very helpful for electronically challenging chemical systems such as free-radicals where the standard MP2 method

dramatically fails due to spin-contamination problem. It is demonstrated that for the aromatic radicals considered the $\langle S^2 \rangle$ value of the UHF wave function is about 1.35 au, while that of the DF-OMP2 wave function is about the theoretical value of 0.75 au. Consequently, for challenging chemical systems, one should prefer DF-OMP2 over the standard MP2 as a more robust method with the same computational scaling.

■ ASSOCIATED CONTENT

Supporting Information

Optimized geometries of aromatic radicals, and total and correlation energies for test sets considered. This material is available free of charge via the Internet at http://pubs.acs.org.

■ AUTHOR INFORMATION

Corresponding Author

*Email: ugrbzky@gmail.com.

Notes

The authors declare no competing financial interest.

■ ACKNOWLEDGMENTS

This research was supported by the Scientific and Technological Research Council of Turkey (TÜBİTAK-113Z203). I thank Miss Emine Soydaş for her assistance with some of the test computations.

■ REFERENCES

(1) Scuseria, G. E.; Schaefer, H. F. *Chem. Phys. Lett.* **1987**, *142*, 354−358.
(2) Sherrill, C. D.; Krylov, A. I.; Byrd, E. F. C.; Head-Gordon, M. *J. Chem. Phys.* **1998**, *109*, 4171−4181.
(3) Bozkaya, U.; Turney, J. M.; Yamaguchi, Y.; Schaefer, H. F.; Sherrill, C. D. *J. Chem. Phys.* **2011**, *135*, 104103.
(4) Bozkaya, U. *J. Chem. Phys.* **2011**, *135*, 224103.
(5) Bozkaya, U.; Schaefer, H. F. *J. Chem. Phys.* **2012**, *136*, 204114.
(6) Soydaş, E.; Bozkaya, U. *J. Chem. Theory Comput.* **2013**, *9*, 1452−1460.
(7) Bozkaya, U.; Sherrill, C. D. *J. Chem. Phys.* **2013**, *138*, 184103.
(8) Bozkaya, U.; Sherrill, C. D. *J. Chem. Phys.* **2013**, *139*, 054104.
(9) Bozkaya, U. *J. Chem. Phys.* **2013**, *139*, 104116.
(10) Soydaş, E.; Bozkaya, U. *J. Chem. Theory Comput.* **2013**, *9*, 4679−4683.
(11) Bozkaya, U. *J. Chem. Phys.* **2013**, *139*, 154105.
(12) Bozkaya, U. *J. Chem. Theory Comput.* **2014**, *10*, 2041−2048.
(13) Soydaş, E.; Bozkaya, U. *J. Comput. Chem.* **2014**, *35*, 1073−1081.
(14) Bozkaya, U. *J. Chem. Theory Comput.* **2014**, *10*, 2371−2378.
(15) Krylov, A. I.; Sherrill, C. D.; Byrd, E. F. C.; Head-Gordon, M. *J. Chem. Phys.* **1998**, *109*, 10669−10678.
(16) Krylov, A. I.; Sherrill, C. D.; Head-Gordon, M. *J. Chem. Phys.* **2000**, *113*, 6509−6527.
(17) Gwaltney, S. R.; Sherrill, C. D.; Head-Gordon, M.; Krylov, A. I. *J. Chem. Phys.* **2000**, *113*, 3548−3560.
(18) Köhn, A.; Olsen, J. *J. Chem. Phys.* **2005**, *122*, 084116.
(19) Lochan, R. C.; Head-Gordon, M. *J. Chem. Phys.* **2007**, *126*, 164101.
(20) Neese, F.; Schwabe, T.; Kossmann, S.; Schirmer, B.; Grimme, S. *J. Chem. Theory Comput.* **2009**, *5*, 3060−3073.
(21) Kurlancheek, W.; Head-Gordon, M. *Mol. Phys.* **2009**, *107*, 1223−1232.
(22) Kossmann, S.; Neese, F. *J. Phys. Chem. A* **2010**, *114*, 11768.
(23) Sokolov, A. Y.; Schaefer, H. F. *J. Chem. Phys.* **2013**, *139*, 204110.
(24) Robinson, J. B.; Knowles, P. J. *J. Chem. Theory Comput.* **2012**, *8*, 2653−2660.
(25) Robinson, J. B.; Knowles, P. J. *J. Chem. Phys.* **2013**, *138*, 074104.
(26) Whitten, J. L. *J. Chem. Phys.* **1973**, *58*, 4496−4501.
(27) Dunlap, B. I.; Connolly, J. W. D.; Sabin, J. R. *J. Chem. Phys.* **1979**, *71*, 3396−3402.
(28) Feyereisen, M.; Fitzgerald, G.; Komornicki, A. *Chem. Phys. Lett.* **1993**, *208*, 359−363.
(29) Vahtras, O.; Almlöf, J.; Feyereisen, M. W. *Chem. Phys. Lett.* **1993**, *213*, 514−518.
(30) Rendell, A. P.; Lee, T. J. *J. Chem. Phys.* **1994**, *101*, 400−408.
(31) Weigend, F. *Phys. Chem. Chem. Phys.* **2002**, *4*, 4285−4291.
(32) Sodt, A.; Subotnik, J. E.; Head-Gordon, M. *J. Chem. Phys.* **2006**, *125*, 194109.
(33) Werner, H.-J.; Manby, F. R.; Knowles, P. J. *J. Chem. Phys.* **2003**, *118*, 8149−8160.
(34) DePrince, A. E.; Sherrill, C. D. *J. Chem. Theory Comput.* **2013**, *9*, 2687−2696.
(35) Beebe, N. H. F.; Linderberg, J. *Int. J. Quantum Chem.* **1977**, *12*, 683−705.
(36) Roeggen, I.; Wisloff-Nilssen, E. *Chem. Phys. Lett.* **1986**, *132*, 154−160.
(37) Koch, H.; de Meras, A. S.; Pedersen, T. B. *J. Chem. Phys.* **2003**, *118*, 9481−9484.
(38) Aquilante, F.; Pedersen, T. B.; Lindh, R. *J. Chem. Phys.* **2007**, *126*, 194106.
(39) Aquilante, F.; Lindh, R.; Pedersen, T. B. *J. Chem. Phys.* **2008**, *129*, 034106.
(40) Turney, J. M.; et al. *WIREs Comput. Mol. Sci.* **2012**, *2*, 556−565.
(41) Shavitt, I.; Bartlett, R. J. *Many-Body Methods in Chemistry and Physics*, 1st ed.; Cambridge Press: New York, 2009; pp 54−89.
(42) Crawford, T. D.; Schaefer, H. F. *Rev. Comp. Chem.* **2000**, *14*, 33−136.
(43) Dalgaard, E.; Jørgensen, P. *J. Chem. Phys.* **1978**, *69*, 3833−3844.
(44) Shepard, R. *Adv. Chem. Phys.* **1987**, *69*, 63−200.
(45) Shepard, R. In *Modern Electronic Structure Theory Part I*; Yarkony, D. R., Ed., 1st ed.; Advanced Series in Physical Chemistry Vol. 2; World Scientific Publishing Company: London, 1995; pp 345−458.
(46) Bozkaya, U. *J. Chem. Phys.* **2014**, *141*, 124108.
(47) Helgaker, T. U.; Almlöf, J. *Int. J. Quantum Chem.* **1984**, *26*, 275−291.
(48) Helgaker, T. U. In *Geometrical Derivatives of Energy Surfaces and Molecular Properties*; Jørgensen, P., Simons, J., Eds.; Springer: Reidel, Dordrecht, 1986; pp 1−16.
(49) Helgaker, T.; Jørgensen, P. *Adv. Quantum Chem.* **1988**, *19*, 183−245.
(50) Simons, J.; Jørgensen, P.; Helgaker, T. U. *Chem. Phys.* **1984**, *86*, 413−432.
(51) Helgaker, T. In *The Encyclopedia of Computational Chemistry*; Schleyer, P. R., Allinger, N. L., Clark, T., Gasteiger, J., Kollman, P. A., Schaefer, H. F., Schreiner, P. R., Eds.; Wiley: Chichester, 1998; pp 1157−1169.
(52) Yamaguchi, Y.; Osamura, Y.; Goddard, J. D.; Schaefer, H. F. *A New Dimension to Quantum Chemistry: Analytic Derivative Methods in Ab Initio Molecular Electronic Structure Theory*; Oxford University Press: New York, 1994; pp 29−52.
(53) Jørgensen, P.; Helgaker, T. *J. Chem. Phys.* **1988**, *89*, 1560−1570.
(54) Helgaker, T.; Jørgensen, P.; Handy, N. *Theor. Chem. Acc.* **1989**, *76*, 227−245.
(55) Helgaker, T.; Jørgensen, P. *Theor. Chem. Acc.* **1989**, *75*, 111−127.
(56) Rice, J. E.; Amos, R. D. *Chem. Phys. Lett.* **1985**, *122*, 585−590.
(57) Yamaguchi, Y.; Schaefer, H. F. In *Handbook of High-Resolution Spectroscopies*; Quack, M., Merkt, F., Eds.; John Wiley & Sons: New York, 2011; pp 325−362.
(58) Weigend, F.; Köhn, A.; Hättig, C. *J. Chem. Phys.* **2002**, *116*, 3175−3183.
(59) Chen, W.; Schlegel, H. B. *J. Chem. Phys.* **1994**, *101*, 5957−5968.
(60) Purvis, G. D.; Sekino, H.; Bartlett, R. J. *Collect. Czech. Chem. Commun.* **1988**, *53*, 2203−2213.
(61) Jurečka, P.; Šponer, J.; Černyá, J.; Hobza, P. *Phys. Chem. Chem. Phys.* **2006**, *8*, 1985−1993.

(62) Dunning, T. H. *J. Chem. Phys.* **1989**, *90*, 1007−1023.
(63) Woon, D. E.; Dunning, T. H. *J. Chem. Phys.* **1995**, *103*, 4572−4585.
(64) Purvis, G. D.; Bartlett, R. J. *J. Chem. Phys.* **1982**, *76*, 1910−1918.
(65) Raghavachari, K.; Trucks, G. W.; Pople, J. A.; Head-Gordon, M. *Chem. Phys. Lett.* **1989**, *157*, 479−483.
(66) Bartlett, R. J.; Watts, J. D.; Kucharski, S. A.; Noga, J. *Chem. Phys. Lett.* **1990**, *165*, 513−522.
(67) Becke, A. D. *J. Chem. Phys.* **1993**, *98*, 5648−5652.
(68) Lee, C.; Yang, W.; Parr, R. G. *Phys. Rev. B* **1988**, *37*, 785−789.
(69) Bozkaya, U.; Özkan, I. *J. Org. Chem.* **2012**, *77*, 2337−2344.
(70) Bozkaya, U.; Özkan, I. *J. Phys. Chem. A* **2012**, *116*, 2309−2321.
(71) Bozkaya, U.; Özkan, I. *J. Phys. Chem. A* **2012**, *116*, 3274−3281.
(72) Bozkaya, U.; Özkan, I. *J. Org. Chem.* **2012**, *77*, 5714−5723.
(73) Bozkaya, U.; Özkan, I. *Phys. Chem. Chem. Phys.* **2012**, *14*, 14282−14292.
(74) Bozkaya, U.; Turney, J. M.; Yamaguchi, Y.; Schaefer, H. F. *J. Chem. Phys.* **2012**, *136*, 164303.
(75) Bozkaya, U.; Turney, J. M.; Yamaguchi, Y.; Schaefer, H. F. *J. Chem. Phys.* **2010**, *132*, 064308.
(76) Neese, F. *WIREs Comput. Mol. Sci.* **2012**, *2*, 73−78.
(77) Thomas, J. R.; DeLeeuw, B. J.; Vacek, G.; Crawford, T. D.; Yamaguchi, Y.; Schaefer, H. F. *J. Chem. Phys.* **1993**, *99*, 403−416.